Journal of Materials Science & Technology 33 (2017) 758–761

Contents lists available at ScienceDirect

Journal of Materials Science & Technology

journal homepage: www.jmst.org

Gradient Structured Copper by Rotationally Accelerated Shot Peening

X. Wang [1], Y.S. Li [1,*], Q. Zhang [2], Y.H. Zhao [1], Y.T. Zhu [1,3]

[1] Nano Structural Materials Center, School of Materials Science and Engineering, Nanjing University of Science and Technology, Nanjing 210094, China
[2] School of Mechanical Engineering, Nanjing University of Science and Technology, Nanjing 210094, China
[3] Department of Materials Science and Engineering, North Carolina State University, Raleigh, NC 27695, USA

ARTICLE INFO

Article history:
Received 21 January 2016
Received in revised form 16 March 2016
Accepted 1 April 2016
Available online 17 November 2016

Key words:
Microstructure
Rotationally accelerated shot peening
Gradient structure
Hardness
Copper

ABSTRACT

A new technology—rotationally accelerated shot peening (RASP), was developed to prepare gradient structured materials. By using centrifugal acceleration principle and large steel balls, the RASP technology can produce much higher impact energy compared to conventional shot peening. As a proof-of-concept demonstration, the RASP was utilized to refine the surface layer in pure copper (Cu) with an average grain size of 85 nm. The grain size increases largely from surface downwards the bulk, forming an 800 μm thick gradient-structured surface layer and consequently a micro-hardness gradient. The difference between the RASP technology and other established techniques in preparing gradient structured materials is discussed. The RASP technology exhibits a promoting future for large-scale manufacturing of gradient materials.

1. Introduction

Gradient structures with excellent mechanical properties have been found in many biological systems such as bamboo and seashells[1]. Several techniques have been developed to prepare gradient materials such as wire brushing[2], ultrasonic shot peening (USP)[3], surface mechanical attrition treatment (SMAT)[4], surface nanocrystallization and hardening (SNH)[5], and surface mechanical grinding treatment (SMGT)[6]. Gradient structures with a grain size varying systematically from nanometer to micrometer induced by these techniques showed many superior properties over conventional homogeneously-structured materials, such as low nitriding temperature[7], excellent tribological properties[8], great fatigue life[9], and good combination of high strength and ductility[10–12]. However, some challenges exist in the industrial application of these technologies. For example, the thickness of gradient layer formed by wire brushing is usually limited. The energy of the balls in USP, SMAT and SNH is controlled by changing the vibration frequency but the velocity of balls cannot be easily controlled. The emerging SMGT technology is quite promising but it is only suitable for cylindrical samples. In summary, development of new technologies is still a challenge to produce gradient structured materials.

Centrifugal force has been widely used in daily life and advanced technology development. For example, it has been used in washing machines, simultaneous densification of intermetallic[13] or even for measurement of xylem cavitation[14]. In this work, based on the centrifugal acceleration principle, a new technology, rotationally accelerated shot peening (RASP) was developed to produce gradient structures on metallic materials, and pure copper (Cu) was chosen as a model material to prove the concept of the RASP technology.

2. Experimental

Experimental setup of the RASP process is illustrated in Fig. 1, mainly containing a power generator, sample room, a steel ball recycle system, a dust elimination system and a control system. Steel balls enter into the rotational system to be accelerated to a high speed by the centrifugal force, and fly off to collide with the surface of a metal sample. Diameter of the balls can be chosen in the range of 1 to 8 mm. Velocity of the steel balls is controlled through rotational speed up to 80 m s^{-1}, which also contributes to the treatment uniformity and coverage. The steel balls are recyclable and can be returned to a storage tank when RASP process is finished. Any contamination produced during RASP process can be eliminated by a dust elimination system. Treated samples are clamped and put in the sample room and can be rotated 360° around the fixed axis. A program can be set with relevant parameters to run the entire RASP process automatically.

* Corresponding author. Fax: +86 25 8430 3281;
E-mail address: liyusheng@njust.edu.cn (Y.S. Li).

http://dx.doi.org/10.1016/j.jmst.2016.11.006
1005-0302/

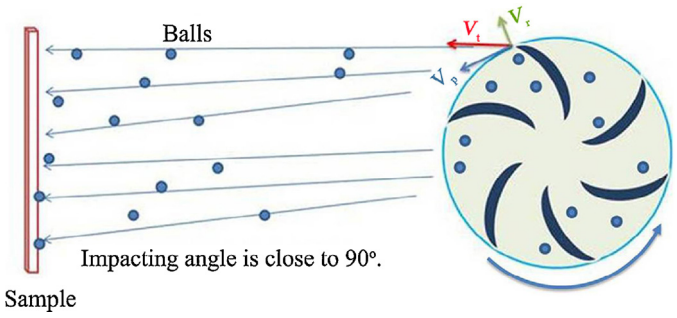

Fig. 1. Schematic illustration of the RASP process.

A commercial 99.97% pure Cu plate (90 mm × 50 mm × 10 mm) was selected as the model material for processing by RASP. The initial grain size was about 100 μm. The sample was treated in open air at room temperature with 3-mm diameter GGr15 steel balls at a velocity of about 25 m s^{-1} for 30 min. The sample was fixed without rotation. An optical microscope (ZEISS AXIO CSM700) was used to observe microstructure of the treated Cu. The microhardness profile from surface to interior in the as-prepared Cu was measured using a HMV-705 tester and the spacing between two indentions is three times greater than the value of indention to avoid overlaps of hardening zones of adjacent indents. Electron Back-Scattered Diffraction (EBSD) observation was carried at a Quant 250 FEG scanning electron microscope (SEM). The step size was 50 nm and the scanning voltage was 20 kV. Cross-sectional microstructure of the treated sample was characterized by using a TECNAI G2 20 LaB6 transmission electron microscope (TEM) at an accelerated voltage of 200 kV. TEM samples were cut by electric spark from the cross section and mechanically polished to 40 μm thick foils. The final thinning was accomplished by ion milling.

3. Results and Discussion

Fig. 2 shows an optical cross-sectional image of RASP-processed Cu. It is apparent that there is a microstructural gradient from surface to interior, though it is hard to differentiate individual grains in the top 100 μm layer, which implies a heavy plastic deformation-induced grain refinement. The initial equiaxed coarse grains become elongated, which can be attributed to the compressive strain induced by the impact of steel balls[15]. Thickness of the gradient layer was estimated to be around 800 μm, which is consistent with the hardness results (Fig. 3). Every hardness datum point is a mean value of 7 replicates with statistical error bar. The average hardness in 10 μm depth from the surface is about 144 HV,

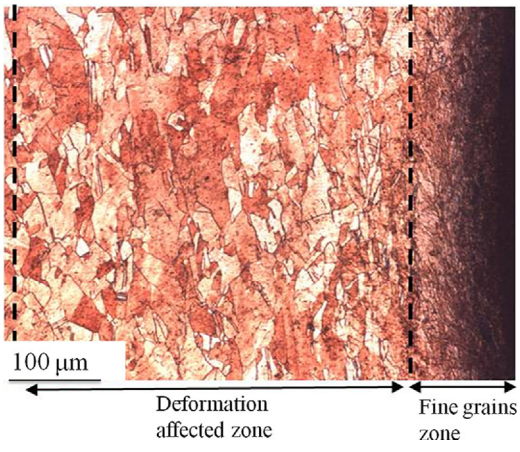

Fig. 2. Optical micrograph of the cross section of a RASP-processed Cu sample.

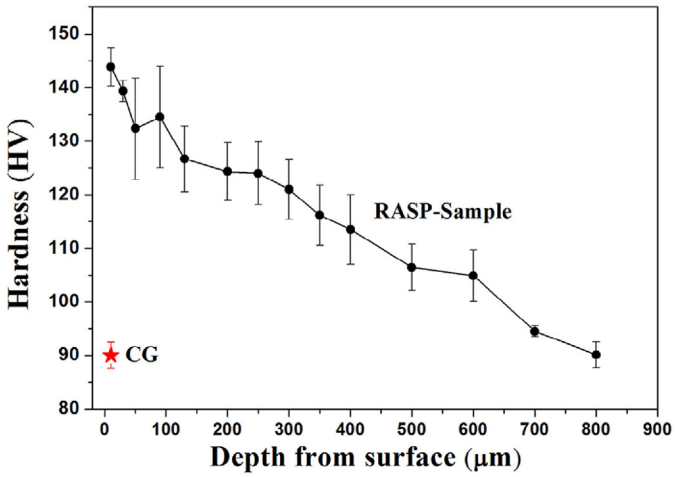

Fig. 3. Hardness gradient as a function of the depth of a RASP-processed Cu sample.

which is significantly higher than that of coarse-grained (CG) sample, which is about 90 HV as indicated by the red star. As shown in Fig. 3, the hardness decreases gradually with distance from surface, and finally approaches to that of CG counterpart (90 HV) at a depth of 800 μm.

To reveal the microstructure of the top surface layer of the RASP-processed Cu sample, EBSD observation was performed. Fig. 4 shows the variation of grain size and orientation along the depth. The black layer corresponds to the layer of nanograins where high strain concentration and fine grains make it impossible to index individual grains correctly[16]. The fraction of grains that can be indexed increases with the distance from surface. Some ultrafine grains are observed in the deeper region. As shown, the grains at larger depth are elongated with the long axis parallel to the sample surface. As discussed above, this is caused by the compressive stress and strain imparted by the colliding steel balls during the RASP process.

Fig. 5(a, b) shows representative cross-sectional TEM bright and dark field micrographs from the top surface of the RASP-processed Cu sample, where a larger number of nanometer-sized grains can be observed and the crystallographic orientations of these nanometer-sized grains are randomly distributed, as indicated by the corresponding selected area electro diffraction (SAED) pattern (Fig. 5(a), inset). The statistical distribution of grain size and aspect ratio is shown in Fig. 5(c, d), as a result of counting 200 grains. The grain size distribution can be described as a normal logarithmic distribution with an average of 85 nm in transverse grain size and 136 nm in longitudinal axis.

Microstructure at different depths was characterized and shown in Fig. 6. From the nano grains in the surface layer (Fig. 5) to the ultrafine grains at the depth of 50 μm and the mixture structures of elongated grains and ultrafine grains at 130 μm (Fig. 6(a, b)), dislocation band structures are formed at the depth of 200 μm (Fig. 6(c)), and finally dislocation cell structure at the depth of 300 μm (Fig. 6(d)), as can be clearly seen that a grain/cell size gradient is formed in the surface of Cu samples induced by RASP treatment. This finding is in agreement with the micro-hardness gradient (Fig. 3), implying that the hardness improvement in RASP-processed Cu mainly comes from the grain refinement and dislocation accumulation. Dislocation cells and walls are formed in the early stage of deformation corresponding to the deeper region (300 μm). Dislocation cell boundaries evolve into low-angle grain boundaries and eventually into high-angle boundaries with increasing strain, which is dominated by dislocation activities[17,18]. The grain refinement and microstructural evolution in Cu during RASP will be further investigated in the future work.

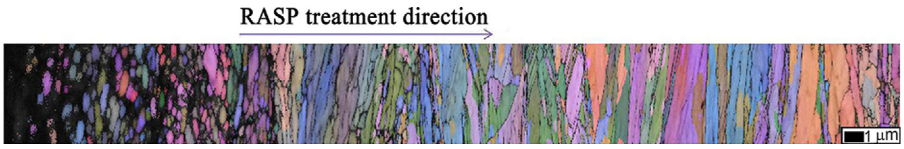

Fig. 4. EBSD mapping graph along the depth of a RASP-processed Cu sample.

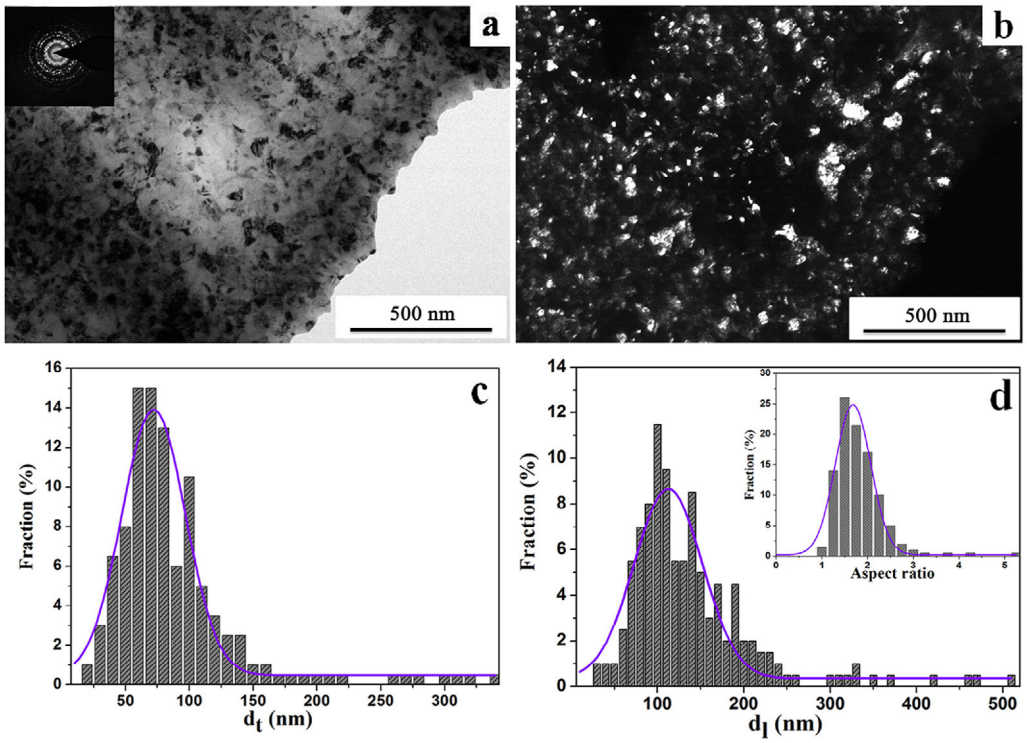

Fig. 5. Representative TEM images of nanometer-sized grains in the top surface layer: (a) Bright field image and SAED pattern (inset); (b) dark field image; (c) histograms of transverse grain sizes (d_t) and (d) longitudinal grain sizes (d_l). The inset in (d) is the aspect ratio (d_t/d_l) distribution.

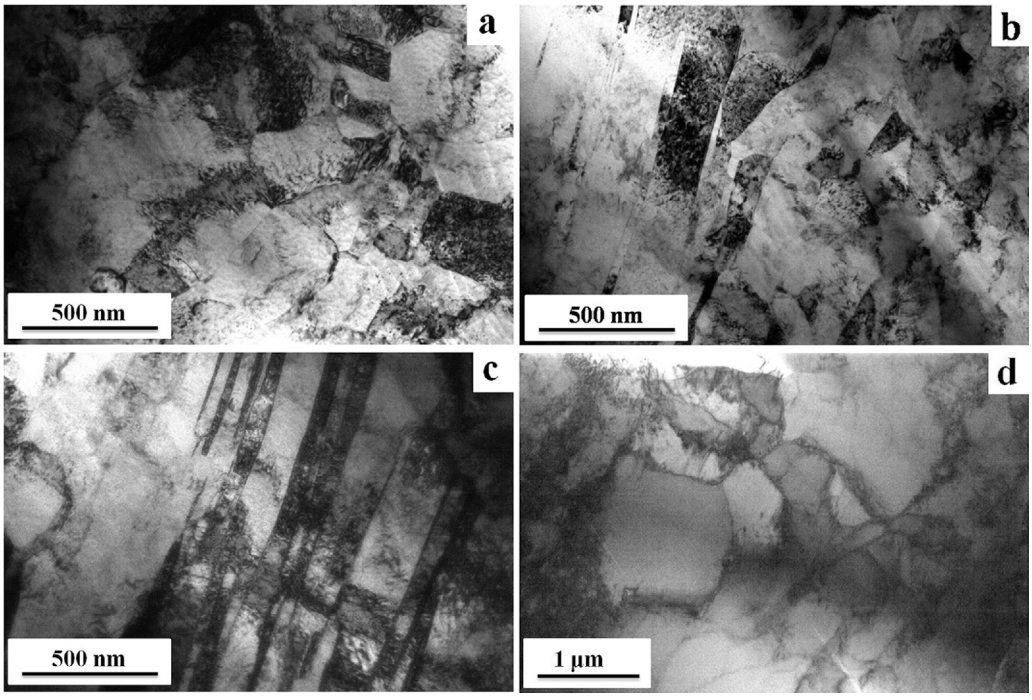

Fig. 6. Microstructure at different depths from surface: (a) 50 μm, (b) 130 μm, (c) 200 μm, and (d) 300 μm.

Table 1
Comparison of process parameters between RASP and other techniques

Technique	Diameter of balls or shots (mm)	Impact velocity (m s^{-1})	Density of balls (g cm^{-3})	Kinetic energy of balls (J)
Shot Peening[19]	0.25–1	20–150	7.74	3.2×10^{-5}–0.12
USP[20,21]	3–7.5	<20	7.98	0.06–0.9
SMAT[22,23]	3–8	2–5	7.98	6×10^{-4}–0.07
SNH[24]	5–7.9	5	14.5	0.03–0.12
RASP	1–8	5–80	7.8	1.3×10^{-4}–17

The refinement of microstructure is attributed to the severe plastic deformation induced by consecutive impacts of high velocity balls on the sample surface with gradient distribution of strain and strain rate[17]. The RASP technique developed here is different from the conventional shot peening in the utilization of steel balls with large size. It is well known that the kinetic energy of these balls depends on their size and velocity, and Table 1 gives a summary of the process parameters and kinetic energy of balls in shot peening, USP, SMAT, SNH and RASP, respectively. It can be seen that though in conventional shot peening the ball speed can reach as high as 150 m/s, the balls in RASP with larger size can possess 100 times higher impact energy than that of conventional shot peening[25], which gives RASP the capability to refine Cu grains to smaller size and much greater depth than conventional shot peening. The thickness of the gradient layer (800 μm) in RASP-processed Cu is similar to that produced by SMAT[17], as compared in Table 1, which is attributed to the comparative kinetic energy of balls between the present RASP process and the SMAT process[17]. It can be also seen from Table 1 that the kinetic energy of balls in RASP can be varied over a much wider range than other techniques. This is of paramount importance because metals with different hardness may need different impact kinetic energy to produce optimum gradient structure and acceptable surface roughness. The influence of RASP processing parameters on the surface roughness and gradient microstructure of other metallic materials are in progress[26].

The RASP technology developed here is conducive to large-scale industrial processing for the following reasons:

Firstly, the RASP technology has lower energy waste and higher processing efficiency. Relatively larger energy waste was caused by the collision between balls and chamber walls in USP[3], SMAT[4] and SNH[5] as a result of random impacts provided by the vibrator. Moreover, the velocity provided by high-frequency vibration is relatively low (<20 m s^{-1})[25], which implies the treatment efficiency is not very high. Compared to these techniques, relatively lower energy consumption of RASP is realized since energy is mainly provided to generate collisions between balls and work pieces because of relatively low scatter angle. Higher impact velocity of RASP process can improve the energy efficiency.

Secondly, there is no shape restriction for RASP samples. By 360° rotation, work pieces can be simultaneously treated by the RASP technology regardless of their shapes.

Thirdly, the RASP process is similar to conventional shot peening technology, which means that the RASP technology can be easily incorporated into a modified conventional shot peening facility and there is no need to rebuild the production line. Furthermore, RASP technique has a high degree of automation as discussed in section 2, which meets the requirements for large-scale production.

It is found that the grain size in the top surface layer is slightly larger than that was reported in SMAT processed Cu[17,27], where the grain size in topmost surface can be refined to 10 nm. The large grain size in the RASP processed Cu could be generated by the recrystallization during RASP processing[6]. Surface heating occurs due to the deformation-induced heat generation within the sample, ball-to-ball impact, and frictional heating during the repeated impact process[28]. The surface temperature increase has a significant effect on the recrystallization and growth of nano-grains[29,30].

The RASP technique provides a new approach to produce gradient structure in metallic materials. Combining the existing advantages of RASP and the experience from traditional shot peening industries, this new technique, is expected to be easily scaled-up and adapted to industrial production and applications.

4. Conclusions

(1) RASP technology has higher impacting energy and can be adjusted in a wider energy range.
(2) The total thickness of gradient structure is 800 μm in RASP processed Cu. A grain/cell size gradient was observed, from micron-sized dislocation cell, evolved to dislocation band structures, ultra-fine grain and finally averaged 85 nm-sized grain in the top surface.
(3) The hardness of top surface is about 144 HV, which is much higher than in the initial coarse-grained sample, a hardness gradient was observed along with distance from the surface.
(4) RASP processing is expected to be easily scaled-up, which makes it promising for industrial applications.

Acknowledgments

Financial supports from the National Natural Science Foundation of China (Grant No. 51301092) and Pangu Foundation are acknowledged.

References

[1] R.O. Ritchie, Nat. Mater 10 (2011) 817–822.
[2] M. Sato, N. Tsuji, Y. Minamino, Y. Koizumi, Sci. Technol. Adv. Mater 5 (2004) 145–152.
[3] G. Liu, J. Lu, K. Lu, Mater. Sci. Eng. A Struct. Mater 286 (2000) 91–95.
[4] K. Lu, J. Lu, J. Mater. Sci. Technol 15 (1999) 193–197.
[5] K. Dai, J. Villegas, L. Shaw, Scr. Mater 52 (2005) 259–263.
[6] W.L. Li, N.R. Tao, K. Lu, Scr. Mater 59 (2008) 546–549.
[7] W.P. Tong, N.R. Tao, Z.B. Wang, J. Lu, K. Lu, Science 299 (2003) 686–688.
[8] Y.S. Zhang, Z. Han, K. Wang, K. Lu, Wear 260 (2006) 942–948.
[9] T. Roland, D. Retraint, K. Lu, J. Lu, Scr. Mater 54 (2006) 1949–1954.
[10] T.H. Fang, W.L. Li, N.R. Tao, K. Lu, Science 331 (2011) 1587–1590.
[11] X. Wu, P. Jiang, L. Chen, F. Yuan, Y.T. Zhu, Proc. Natl. Acad. Sci. U.S.A. 111 (2014) 7197–7201.
[12] X.L. Wu, P. Jiang, L. Chen, J.F. Zhang, F.P. Yuan, Y.T. Zhu, Mater. Res. Lett 2 (2014) 185–191.
[13] R. Seshadri, Mater. Manuf. Process 17 (2002) 501–518.
[14] N.N. Alder, W.T. Pockman, J.S. Sperry, S. Nuismer, J. Exp. Bot 48 (1997) 665–674.
[15] Y.S. Li, N.R. Tao, K. Lu, Acta Mater 56 (2008) 230–241.
[16] Y. Samih, B. Beausir, B. Bolle, T. Grosdidier, Mater. Charact 83 (2013) 129–138.
[17] K. Wang, N.R. Tao, G. Liu, J. Lu, K. Lu, Acta Mater 54 (2006) 5281–5291.
[18] J. Huang, Y. Zhu, H. Jiang, T. Lowe, Acta Mater 49 (2001) 1497–1505.
[19] Y.F. Al-Obaid, Mech. Mater 19 (1995) 251–260.
[20] N.R. Tao, M.L. Sui, J. Lu, K. Lua, Nanostruct. Mater 11 (1999) 433–440.
[21] X. Wu, N. Tao, Y. Hong, B. Xu, J. Lu, K. Lu, Acta Mater 50 (2002) 2075–2084.
[22] N. Tao, Z. Wang, W. Tong, M. Sui, J. Lu, K. Lu, Acta Mater 50 (2002) 4603–4616.
[23] K.Y. Zhu, A. Vassel, F. Brisset, K. Lu, J. Lu, Acta Mater 52 (2004) 4101–4110.
[24] K. Dai, J. Villegas, Z. Stone, L. Shaw, Acta Mater 52 (2004) 5771–5782.
[25] K. Dai, L. Shaw, Mater. Sci. Eng. A Struct. Mater 463 (2007) 46–53.
[26] X. Wang, Y.S. Li, Mater. Lett (2016), submitted.
[27] J. Guo, K. Wang, L.U. Lei, J. Mater. Sci. Technol 22 (2006) 789–792.
[28] K.A. Darling, M.A. Tschopp, A.J. Roberts, J.P. Ligda, L.J. Kecskes, Scr. Mater 69 (2013) 461–464.
[29] M. Ames, J. Markmann, R. Karos, A. Michels, A. Tschöpe, R. Birringer, Acta Mater 56 (2008) 4255–4266.
[30] G. Sharma, J. Varshney, A.C. Bidaye, J.K. Chakravartty, Mater. Sci. Eng. A Struct. Mater 539 (2012) 324–329.